

See discussions, stats, and author profiles for this publication at:
<https://www.researchgate.net/publication/223410684>

Prediction of water quality in lakes and reservoirs. Part I – Model description

Article in *Ecological Modelling* · March 1997

DOI: 10.1016/S0304-3800(96)00062-2

CITATIONS

267

READS

645

2 authors:



David Philip Hamilton

The University of Waikato

270 PUBLICATIONS **4,308** CITATIONS

[SEE PROFILE](#)



S. Geoffrey Schladow

University of California, Davis

139 PUBLICATIONS **2,856** CITATIONS

[SEE PROFILE](#)

Some of the authors of this publication are also working on these related projects:



PhD Research on Oligopeptides from Aquatic Cyanobacteria [View project](#)



Lake Tahoe limnology [View project](#)

All content following this page was uploaded by [David Philip Hamilton](#) on 08 August 2014.

The user has requested enhancement of the downloaded file.

Prediction of water quality in lakes and reservoirs. Part I – Model description

David P. Hamilton ^{*}, S. Geoffrey Schladow ¹

Department of Environmental Engineering, Centre for Water Research, The University of Western Australia, Nedlands WA 6907, Australia

Received 3 November 1995; accepted 27 June 1996

Abstract

A one-dimensional water quality model (DYRESM Water Quality) is described which combines a process based hydrodynamic model (DYRESM) with numerical descriptions of phytoplankton production, nutrient cycling, the oxygen budget and particle dynamics. The hydrodynamic component is free from calibration, which ensures that it is readily transferable to other lakes and reservoirs. This improves water quality predictions derived for different hydrodynamic forcing events. It also allows for identification of the specific hydrodynamic processes that influence water quality. The water quality component consists of 13 state variables which may include up to three algal groups, BOD, dissolved oxygen and four components of the dissolved oxygen budget (inflows, biochemical processes, surface aeration and oxygen present in the reservoir at the start of a simulation), nutrients ($\text{PO}_4\text{-P}$, $\text{NO}_3\text{-N}$, $\text{NH}_4\text{-N}$, TP and TN) and inorganic particles. The particle model simulates settling and flocculation/deflocculation of up to seven different size classes of particles. The hydrodynamic, water quality and particle models interact on a sub-daily time step. Forcing data for the model are entered as daily-averaged values. The ecological component requires calibration for each new application through adjustment of several different biological and chemical parameters. Literature ranges for these parameters are wide, but provided the process description is correct, many of the parameters can be validated with measured data. © 1997 Elsevier Science B.V.

Keywords: Lake and reservoir model; DYRESM Water Quality; Ecological parameters; Vertical density stratification

1. Introduction

The need for predictive water quality modelling has arisen largely as a result of increased eutrophication of lakes throughout the world (Forsberg, 1987; Canfield and Hoyer, 1988). The most common modelling approach is exemplified by the development and application of steady state, input–output models

(see reviews by Mueller, 1982; Ahlgren et al., 1988). Generally, nutrient concentrations are calculated from net inputs and chlorophyll *a* concentration (or another indicator of phytoplankton biomass) is predicted by correlation with the limiting nutrient, most often phosphorus (Dillon and Rigler, 1975; Canfield and Bachmann, 1981; OECD, 1982). Factors that can also influence phytoplankton biomass, such as light climate, biological interactions and internal loading of nutrients, are not considered. Furthermore, the assumption that a lake is a continuously mixed system is very restrictive and only applicable at discrete times of the year, if at all (Imberger and

^{*} Corresponding author. Tel.: +61-9-3803530; fax: +61-9-3801015.

¹ Present address: Department of Civil and Environmental Engineering, University of California, Davis, CA 95616, USA.

Patterson, 1990). As a result, the shortcomings of such approaches include an inability to make predictions in the face of varying physical and biological conditions, and a failure to offer insights into the determinants of changing water quality.

A second approach, often referred to as ecological water quality modelling, specifically addresses many of the biological and chemical factors that are absent in the simple input–output models. This approach has evolved in order to obtain a more fundamental understanding and representation of the major physical, chemical and biological processes that affect the biomass of phytoplankton and higher trophic levels (e.g. Di Toro et al., 1971; Scavia, 1980; Jørgensen, 1983; Matsuoka et al., 1986). Typically such models represent ecological processes by time varying, interdependent conservation equations, with rate coefficients that require calibration to suit site-specific conditions. The need for site-specific calibration is an undesirable feature of these models. However, present understanding does not afford a more fundamental, calibration-free description of the range of processes covered.

In ecological water quality models, the physical processes of transport and mixing within the water body have generally been oversimplified, with the assumption of a continuously stirred or two compartment vertical system being common. Interactions between physical processes and the biological and chemical processes described by these models are thus poorly represented. The predictive abilities of these models are therefore compromised, despite increased ability to simulate the response to a range of altered biological and chemical conditions.

A third approach has been the extension of hydrodynamic models to include water quality components, either by combination with simple input–output models or more recently with ecological models. Orlob (1983) and Watanabe et al. (1983) review the evolution of such models. The most common approach for the hydrodynamics has been to use a one-dimensional (1D) model, with retention of variations in the vertical dimension. Many of the early, widely used models are not process based, and instead solve the 1D, thermal advection–diffusion equation (Dake and Harleman, 1966; Orlob and Selna, 1970). The calibration required for the hydrodynamic model, when coupled with the calibration of

the biochemical component of the model, is very limiting and the results are of questionable value when predictions are required under conditions of changed inputs.

Three process based, hydrodynamic models are those of Stefan and Ford (1975), Bloss and Harleman (1980), and Imberger et al. (1978). The first two have been coupled with ecological models, giving the water quality models MINLAKE (Riley and Stefan, 1987; Riley and Stefan, 1988) and CE-QUAL (USCE, 1986) respectively. All three hydrodynamic models present a description of the mixing and transport processes associated with inflow, outflow, diffusion and mixed layer dynamics. The models differ most in the extent to which the individual processes are described. The mixed layer dynamics, arguably the most important process in terms of algal production, provide the best example. Each model recognizes the production of turbulent kinetic energy (TKE) as the basis of the description of mixed layer deepening. The Stefan and Ford model relates the total TKE production to the observed mixed layer deepening via an adjustable parameter. The Bloss and Harleman model divides the TKE production into two components, with one of these adjustable to allow for different mixing efficiencies under different levels of stratification and wind stress. The Imberger et al. model, DYRESM, computes the TKE produced through four discrete processes. The amount of mixing is at a fixed rate for each process, having been determined independently from consideration of theoretical, laboratory and field results (e.g. Imberger and Patterson, 1981).

The fact that only the Imberger et al. (1978) model is free of calibration, implies that the level of process description, including the temporal and spatial scales in the model, is fundamentally correct. This result has been confirmed by the application of the model to a large number of lakes and reservoirs (Imberger and Patterson, 1990). DYRESM (or more correctly, a later version of it) has therefore been used for the hydrodynamic component of the water quality model described below.

The purpose of the present work is to present a coupled hydrodynamic–ecological water quality model in which the hydrodynamic component is totally calibration free. The hydrodynamics can be one of the dominant factors in lake ecology (Vincent

et al., 1991), so a major advantage of such an approach is that it extends the range of application of the model to cover altered hydrodynamic conditions in which calibration data may not exist. This approach also enables the interactions between ecological and hydrodynamic processes to be examined at a more fundamental level. The DYRESM Water Quality model therefore represents a significant improvement over the few existing models of this type. It is still restricted, however, to calibration of the ecological algorithms. While there has recently been progress made towards mechanistic descriptions of ecological processes (e.g. Jørgensen, 1992; Kmet et al., 1993; Patterson et al., 1994) and in numerically quantifying the values of specific parameters (Jørgensen et al., 1991) present understanding has not evolved to the extent that eutrophication models are completely free from calibration.

We follow an approach similar to that taken in the earlier coupled models, in that we rely on the ecological modelling literature to guide our selection of algorithms that describe the biological and chemical processes. Some of the individual choices described below are identical to those of MINLAKE or CEQUAL, but the coupled water quality model is unique.

In what follows we describe the hydrodynamic model, the particle settling model, and the ecological model that comprise the present water quality model. A description of the calibration procedure adopted for the ecological model, and a comparison between model predictions and field observations is presented in Part II.

2. Water quality model

The model, DYRESM Water Quality (DWQ), comprises a number of components. The hydrodynamic component includes separate algorithms for individual mixed layer processes, inflow (both riverine and groundwater), natural or man-made outflows, and hypolimnetic mixing. The particle settling component allows for the gravitational settling of a spectrum of particle sizes with variable degree of coagulation. The ecological component models phytoplankton production, nutrient cycling, and the dissolved oxygen budget. The following sections describe these components. As some components have been well documented previously, their descriptions will be brief. However, the description is considered necessary to explain the functioning of DWQ. Descriptions are also given of the model architecture, time stepping, spatial discretization, input data requirements, and output.

2.1. Spatial discretization

The spatial discretization is identical to that used in the 1D hydrodynamic model DYRESM. The vertical profile of the lake is represented as a set of up to 100 Lagrangian layers which are free to move vertically, and to contract and expand in response to inflows, outflows and surface mass fluxes. The Lagrangian formulation avoids the need to calculate vertical velocities, greatly decreasing computational time and minimizing numerical diffusion. Each layer is homogeneous, and property differences between

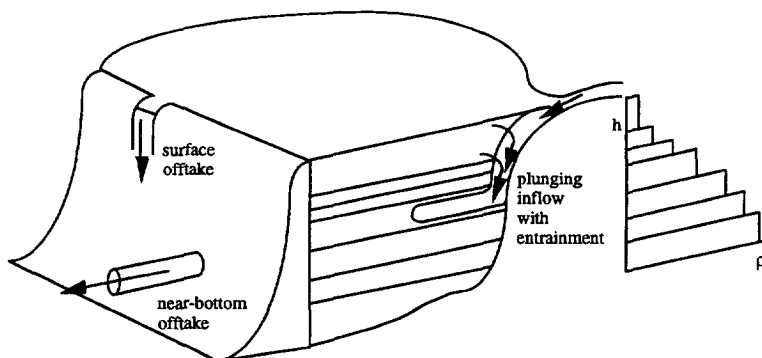


Fig. 1. Schematic representation of the layer structure showing the relation between height above the bottom (h) and density (ρ).

layers represent the vertical distribution. Layer thicknesses are adjusted within the model according to the resolution required to represent the vertical density gradient. The model is initialized with measured data for each layer. Fig. 1 shows the schematic representation of the layer structure.

Mixing is represented by the amalgamation of layers. Properties of the amalgamated layer are volumetrically averaged, and the total number of model layers is decreased accordingly. Amalgamated layers may be split according to a specified maximum layer thickness criterion. Conversely, when a layer size falls below a specified minimum criterion, as may occur when there is withdrawal of water from the lake, then the layer is amalgamated with the smaller of the two bounding layers.

A unique feature of the spatial discretization is an extension to allow a quasi two-dimensional representation of riverine inflows (Jokela and Patterson, 1985), as it may take several days for inflows to intrude across the full length of larger lakes. It is only when the inflow for a particular day has completely crossed the lake that water from that inflow is added to the 1D layer structure.

2.2. Time step

Just as the spatial discretization varies with the scale of the dominant mixing processes, so too does the temporal scale. Two timesteps characterize the

model. A daily (24 h) timestep is used for inflows and outflows, as neither of these processes varies appreciably on smaller timescales. Within the daily timestep is a variable length, sub-daily timestep. All other processes, both hydrodynamic and water quality, are advanced in parallel at the sub-daily timestep.

The calculation of this sub-daily timestep differs from that used in DYRESM. It is linked to the two major external forcing functions; the thermal transfers and the wind stress. The thermal component is determined as follows. For measured incoming short-wave radiation, a correction is made for albedo (Patten et al., 1975):

$$A_o = 0.08 + 0.02 \left[\frac{2\pi N_d}{365} \pm \frac{\pi}{2} \right] \quad (1)$$

with the term $\pi/2$ added for the Northern Hemisphere and subtracted for the Southern Hemisphere.

The photoperiod (seconds of sunshine in a day) is defined by Kreith and Kreider (1978) as:

$$T_p = \frac{86400}{\pi} \cos^{-1} \left[\tan \left(\pm \frac{\pi L}{180} \right) \right. \\ \left. \times \tan \left[-23.45 \frac{\pi}{180} \sin \left[\frac{2\pi(284 + N_d)}{365} \right] \right] \right] \quad (2)$$

where N_d is the number of days since the beginning of the year and L is the latitude in degrees (positive for Northern Hemisphere and negative for Southern

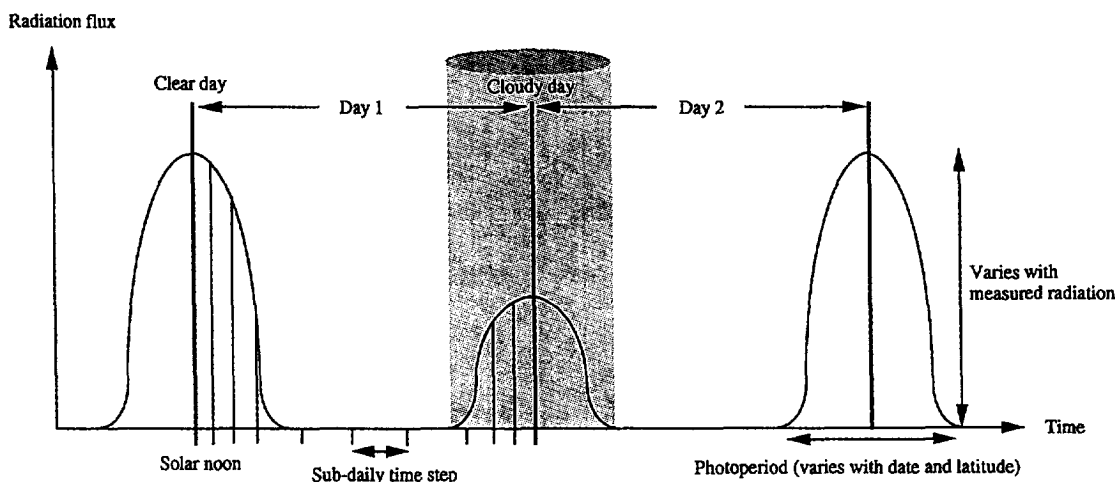


Fig. 2. Representation of shortwave radiation distribution and timesteps used in the model.

Hemisphere). Shortwave radiation is distributed sinusoidally over the photoperiod, with the amplitude varying such that the integrated daily value equals the measured radiation. Cloudy days thus have a low amplitude of radiation and clear days a high amplitude, as shown schematically in Fig. 2.

Shortwave radiation is absorbed with depth in the water column according to a Beer's law formulation. Longwave radiation is assumed to be totally absorbed and emitted by the uppermost layer. When longwave radiation is not measured, it is calculated according to the Stefan-Boltzmann equation, but with adjustments made for surface emissivity in the case of outgoing radiation, and for cloud cover and atmospheric constituents in the case of incoming radiation (Tennessee Valley Authority, 1972). There are also energy fluxes across the water surface due to sensible and latent heat transfers (Tennessee Valley Authority, 1972). Starting at solar noon, the beginning of a day in the model, the length of time (to the nearest 15 min) required to produce a 3°C temperature change in the uppermost model layer is defined as:

$$\Delta t_{th} = 3.0 \rho_s V_s C_p \left/ \left[A_s \left(LW_{net} - E - H + \int_{t_1}^{t_2} \frac{Q_o dt}{t_2 - t_1} \right) - A_{s-1} \int_{t_1}^{t_2} \frac{Q_o e^{-\eta h} dt}{t_2 - t_1} \right] \right. \quad (3)$$

Here ρ is water density, V and A are layer volume and surface area, C_p is the specific heat capacity, LW_{net} is the measured net long-wave flux, E and H are the calculated evaporative and sensible heat fluxes, Q_o is the shortwave radiation flux, η is the light extinction coefficient and h is the surface layer depth. Subscripts s and $s-1$ refer to the surface layer and the layer immediately below it, respectively, and t_1 and t_2 are the time limits of the integration. If this is less than the time to the end of the photoperiod, then it is set as the current thermal timestep. If it exceeds it, then the time to the end of the photoperiod is used instead.

The wind stress timestep is calculated (to the nearest 15 min) as the time required to limit the increase in the shear velocity of the surface layer of the model to 0.1 ms^{-1} . If the acceleration of this layer is given by u_*^2/h , where u_* is the velocity

scale for wind shear and h is the layer thickness, then the timestep is defined as

$$\Delta t_s = \frac{0.1 h}{u_*^2} \quad (4)$$

The actual timestep used in the model is the minimum of the thermal and wind stress timescales, i.e. $\Delta t = \min\{\Delta t_{th}, \Delta t_s\}$. Its minimum length is 15 min, and its maximum length is the total hours of darkness on a particular day. As the shortwave radiation profile and the surface layer properties vary throughout the day, the length of the sub-daily timestep is recalculated at the completion of every timestep.

2.3. Model architecture

Following the initialization of the model and the reading of fixed data (e.g. hypsography), data for the first day of the simulation are read. This allows for the calculation of the sub-daily timestep. The hydrodynamic processes (with the exception of inflows and withdrawals), the particle settling processes, and the water quality processes are advanced on this timestep, resulting in the modification of the layer structure and of the values of layer variables. On completion of the water quality algorithms, the model loops back to the beginning of the hydrodynamic model to calculate the next sub-daily timestep, and the sequence is repeated. This continues until the sub-daily timesteps total 24 h, at which time the inflow and outflow processes operate for a single 24 h timestep. Once complete, the next day's data are read and the entire process repeated.

2.4. Hydrodynamic model

The hydrodynamic model used is the most recent version of DYRESM, a one-dimensional simulation model of the vertical distribution of temperature and salinity in small to medium size lakes and reservoirs (Imberger et al., 1978; Imberger and Patterson, 1981; Patterson et al., 1984). Surface fluxes of momentum, sensible heat and latent heat are computed from bulk aerodynamic formulae for stress, sensible heat transfer, and evaporative heat transfer (Imberger and Patterson, 1990).

Surface layer dynamics are based on an integral

Table 1
List of symbols

Hydrodynamic symbols	
A	layer surface area
A_o	albedo
C_E, C_H, C_W	process-specific bulk aerodynamic transfer coefficients
C_D	stream drag coefficient
C_p	specific heat capacity of water
D_z	turbulent diffusivity coefficient
E	evaporative heat flux
En	inflow entrainment coefficient
F_i	internal Froude Number.
F	Froude Number
g	acceleration due to gravity
Gr	Grashof Number
h	layer thickness
h'	depth of layer immediately below surface layer
h_1	depth from the lake bottom to the centre of area of the N^2 distribution
H	sensible heat flux
H_t	total depth of water
k_o	wave number of the largest eddies
KE_A	available turbulent kinetic energy in the surface layer
L	length of lake at inflow insertion height
La	latitude
LW_{net}	net long-wave radiation flux
LW_o	incoming longwave radiation
N	buoyancy frequency of stream inflow
N	Brunt–Väisälä frequency
N_d	number of days since the beginning of the year
PE_R	required potential energy for mixing in the surface layer
q_A	specific humidity of air
q_S	specific humidity of water surface
Q	volume flux of the insertion
Q_o	shortwave radiation flux at the top of a layer
ρ	water density
ρ_o	reference density
s and $s - 1$	references for surface layer and layer immediately below it
t_1, t_2	references for time limits of integration
T_A	air temperature
T_K	absolute air temperature
T_S	surface water temperature
T_P	photoperiod
τ	wind shear stress
u	withdrawal velocity
u_1	shear velocity at the bottom of the surface layer
u_*	turbulent velocity scale for wind shear
u_o	maximum withdrawal velocity
U	wind speed
V	layer volume
w_*	turbulent velocity scale for penetrative convection
x	horizontal distance relative to the center of the offtake
z	vertical distance relative to the center of the offtake
z_o	height of the offtake
α	constant related to the mixing efficiency of the turbulence
β	half angle of river cross-section
δ	Kelvin–Helmholtz billow thickness scale
$\Delta\rho$	density jump across bottom of surface layer
Δt_{th}	thermal timestep
Δt_s	wind stress timestep

Table 1 (continued)

List of symbols

Δt	timestep
ϵ	dissipation
Φ	riverbed slope
η	light extinction coefficient
λ	withdrawal layer thickness
σ	first moment distance of the N^2 distribution below h_1
ν	kinematic viscosity
ψ, C_K, C_T and C_S	process-specific parameters for mixing efficiency
ζ	Stefan-Boltzmann constant

Biological and chemical symbols

A	area of bottom sediments
BOD	biochemical oxygen demand of detritus
C^*	dissolved oxygen concentration at saturation
DO	dissolved oxygen
E_{gzp}	excretion rate from zooplankton
G_p	maximum rate of phytoplankton growth
I	light intensity
I_s	saturation light intensity
IN	internal nitrogen
IP	internal phosphorus
IN_{max}	maximum internal nitrogen concentration
IN_{min}	minimum internal nitrogen concentration
IP_{max}	maximum internal phosphorus concentration
IP_{min}	minimum internal phosphorus concentration
k_b	rate coefficient sediment oxygen demand
K_b	half saturation constant for dependence of sediment oxygen demand on dissolved oxygen
k_B	rate coefficient for detrital breakdown
K_{BOD}	half saturation constant for dependence of detrital decay on dissolved oxygen
k_d	rate coefficient for denitrification
K_{den}	half saturation constant for dependence of denitrification on dissolved oxygen
K_{gz}	rate coefficient for zooplankton grazing
k_m	rate coefficient for mortality
k_n	rate coefficient for nitrification
K_N	half saturation constant for nitrogen uptake
K_{nit}	half saturation constant for dependence of nitrification on dissolved oxygen
k_{NO}	rate coefficient for nitrification
k_{ON}	rate coefficient for mineralization of nitrogen in organic form
k_{OP}	rate coefficient for mineralization of nitrogen in organic form
K_p	half saturation constant for external phosphorus uptake
k_r	rate coefficient for respiration
K_s	factor regulating sediment nutrient release with dissolved oxygen concentration
K_{PZ}	half saturation constant for zooplankton grazing
NO_3	nitrate
NH_4	ammonium
ON	nitrogen in particulate organic form
OP	phosphorus in particulate organic form
P	phytoplankton as chlorophyll <i>a</i>
PO_4	dissolved reactive phosphorus
S	concentration of suspended sediment
S_N	release rate of ammonium from the sediment
S_p	release rate of phosphorus from the sediment

Table 1 (continued)

List of symbols

U_N	maximum rate of nitrogen uptake
U_P	maximum rate of phosphorus uptake
W	transfer velocity of oxygen at the water surface
Y_{CC}	factor for conversion of chlorophyll <i>a</i> to carbon (Ambrose et al., 1988)
Y_{OC}	factor for conversion of carbon to oxygen produced or consumed
Y_{ON}	stoichiometric ratio of oxygen to nitrogen for nitrification
Z	zooplankton biomass
η_C	specific extinction coefficient for chlorophyll <i>a</i>
η_S	specific extinction coefficient for suspended sediment
η_W	background extinction coefficient
θ_x	temperature multiplier, where <i>x</i> represents the specific biochemical process
ρ_B	density of particulate organic matter
ρ_P	phytoplankton density
ρ_T	density of particulate nutrients

turbulent kinetic energy model (Sherman et al., 1978). The turbulent kinetic energy budget is partitioned between processes of wind stirring, convective overturn, interfacial shear production and Kelvin–Helmoltz billowing. The energy calculated to be available through each of these processes is compared with the potential energy required to combine the layer immediately below. If sufficient energy is available, the layers are combined and the available energy is decreased by the gain in potential energy. The process is repeated until insufficient energy remains within the present time step to continue the deepening process. The parameters for the efficiency of the individual mixing processes are fixed at values derived from theoretical considerations, laboratory experiments and field observations (Sherman et al., 1978; Imberger and Patterson, 1981).

River inflow is modelled in three stages as a quasi two-dimensional process. As the stream enters a lake or reservoir it pushes stagnant lake water ahead of itself until buoyancy forces arrest the flow. At this point, the stream either flows over the lake surface or plunges beneath the surface, depending on the relative densities of the inflow and the lakewater surface. Once submerged, the stream will flow down the lake bottom gradient, entraining ambient water. At its level of neutral buoyancy, the stream and its entrained flow intrude horizontally in a narrow distribution governed by either a gravitational–inertial or a gravitational–viscous balance that depends on a Grashof Number and Froude Number criterion (Im-

berger et al., 1976). The stream inflow for a given day is not inserted into the model Lagrangian layer structure until it intrudes across the full length of the lake (Jokela and Patterson, 1985). Groundwater inflows may be modelled similarly to surface inflows, but with no entrainment (Casamitjana and Schladow, 1993a).

Outflow is accomplished by adjustment of the volumes of the layers that are affected by each withdrawal. For submerged offtakes the thickness of the water that is withdrawn is determined by the stratification, the discharge, and the nature of the offtake (line or point sink), and is governed by similar Grashof and Froude number relationships as for intrusions (Imberger and Patterson, 1990). By integrating backwards along the flow streamlines, an envelope of water withdrawn over each day is produced and the composition of the withdrawn water is determined as a volumetric average of the withdrawn water (Hocking et al., 1988).

Hypolimnetic mixing is modelled by a turbulent diffusivity coefficient, the value of which depends directly on the dissipation of the turbulent kinetic energy and inversely on the stratification (Weinstock, 1981). The dissipation is assumed to be equivalent to the energy input by the wind and decays exponentially from the region of most severe stratification (Imberger, 1982). A list of symbols is given in Table 1 and a summary of the equations for the major hydrodynamic processes described above is given in Table 2.

2.5. Particle model

The particle model simulates settling, aggregation and diffusion for a given distribution of particles in the water column. It has been described in detail by Casamitjana and Schladow (1993b) and is based on the model proposed by O'Melia (1980).

Table 2

List of equations for the hydrodynamic component of the DYRESM Water Quality model. Symbols are given in Table 1

Surface flux of momentum

$$\tau = \rho_A C_E U^2$$

Surface flux of sensible heat

$$H = -\rho_A C_p C_H U (T_A - T_S)$$

Surface flux of evaporative heat

$$E = -\rho_A C_w U (q_A - q_S)$$

Shortwave radiation distribution over depth

$$Q(h) = Q_0 e^{-\eta h}$$

Longwave radiation input to surface layer

$$LW_0 = \zeta T_K^4$$

Available kinetic energy of surface layer

$$KE_A = \frac{C_K}{2} (w_*^3 + \psi^3 u_*^3) \Delta t + \frac{C_S}{2} \left[u_1^2 + \frac{u_1^2}{6} \frac{d\delta}{dh} + \frac{u_1 \delta}{3} \frac{du_1}{dh} \right] h'$$

Required potential energy of surface layer

$$PE_R = \left[\frac{C_T}{2} (w_*^3 + \psi^3 u_*^3)^{2/3} + \frac{\Delta \rho g h}{\rho_0} + \frac{g \delta^2}{24 \rho_0} \frac{d(\Delta \rho)}{dh} + \frac{g \Delta \rho \delta}{12 \rho_0} \frac{d\delta}{dh} \right] h'$$

River inflow entrainment

$$En = \frac{3}{4} \left[\frac{5 \tan \Phi}{F_i^2} - \frac{5 C_D}{\sin \beta} \right] \frac{F_i^2}{(3 F_i^2 + 2)}$$

Grashof Number

$$Gr = N^2 L^4 / \nu^2$$

Froude Number

$$F = Q / N L^2$$

Outflow withdrawal velocity

$$u = 0.5 u_0 \left(1 - \frac{x}{L} \right) \left[1 + \cos \pi \frac{(z - z_0)}{\lambda} \right]$$

Hypolimnetic diffusivity

$$D_z = \frac{\alpha \varepsilon}{N^2 + k_\sigma^2 u_*^2}$$

Brunt-Väisälä frequency

$$N^2 = -\frac{g \partial \rho}{\rho \partial z}$$

Dissipation

$$\varepsilon = \langle \varepsilon \rangle \text{ for } z \geq H_1 - h_1$$

$$\varepsilon = \langle \varepsilon \rangle \exp \left[-\frac{H_1 - h_1 - z}{\sigma} \right]^2 \text{ for } z < H_1 - h_1$$

The distribution of particles of any size can be written as:

$$\frac{\partial n_k}{\partial t} = \frac{1}{2} \sum_{i+j=k} \alpha \lambda(i, j) n_i n_j - n_k \sum_{i=1}^{\infty} \alpha \lambda(i, j) n_i$$

$$- w_k \frac{\partial n_k}{\partial z} + \frac{\partial}{\partial z} \left(A(k, z) \frac{\partial n_k}{\partial z} \right) \quad (5)$$

where n_k is the concentration of particles of size k , α is a collision efficiency factor, reflecting the stability and surface chemistry of the particles, $\lambda(i, j)$ is a collision frequency that depends on contacts between particles of size i and size j , which form particles of size k , w_k is the settling velocity of particles of size k , and $A(k, z)$ is an exchange coefficient, accounting for turbulent and molecular effects.

Contacts between particles can occur by three different processes: Brownian diffusion, fluid shear and differential settling. The collision frequency functions for each of these processes are respectively:

$$\lambda(i, j)^{BR} = \frac{2 K T_K (d_i d_j)^2}{3 \mu d_i d_j} \quad (6)$$

$$\lambda(i, j)^{SH} = \frac{1}{6} (d_i + d_j) \left(\frac{\varepsilon}{\nu} \right)^{1/2} \quad (7)$$

$$\lambda(i, j)^{ST} = \frac{\pi (\rho_P - \rho)}{72 \mu} (d_i + d_j)^3 |d_i - d_j| g \quad (8)$$

Here K is the Boltzmann constant, d is the particle diameter, μ and ν are the absolute viscosity and kinematic viscosity of the water and ρ_P is the density of the particle. The dissipation, ε , is as defined by Eq. (16).

The settling velocity of the particle follows Stokes' equation:

$$w_k = \frac{g (\rho_P - \rho)}{18 \mu} d_k^2 \quad (9)$$

The diffusion coefficient is given by

$$A(k, z) = D_z + D'_k \quad (10)$$

where D'_k is the Stokes–Einstein molecular diffusion coefficient for the particle k (O'Melia, 1990)

$$D'_k = \frac{KT}{3\pi\mu d_k} \quad (11)$$

and D_z is as defined in Table 2.

2.6. Ecological model

The ecological model comprises of subroutines for phytoplankton production and loss, nutrient cycling and dissolved oxygen dynamics. At each sub-daily timestep and in each model layer, the set of equations that describe these processes is solved. At this same timestep, settling, diffusion, mixing and changes in temperature and light can also alter concentrations of each of the ecological state variables in any layer. At the conclusion of each day, inflow and withdrawal processes may change concentrations

of variables in some of the layers by adding or removing water of known concentration. Fig. 3 shows the interrelationships between the main ecological state variables.

2.7. Phytoplankton

Phytoplankton biomass is represented in the model as the concentration of chlorophyll a , either for the entire phytoplankton assemblage, or as the individual contributions by certain groups, e.g., cyanobacteria, diatoms and other phytoplankton such as chlorophytes. A minimum of expressions for limitation by light, internal (cellular) phosphorus, internal nitrogen and, when diatoms are modelled explicitly, silica, is used to constrain the maximum growth potential of phytoplankton (e.g. Larsen et al., 1974; Scavia and Park, 1976; Riley and Stefan, 1987). It should be noted, however, that the interaction of light and

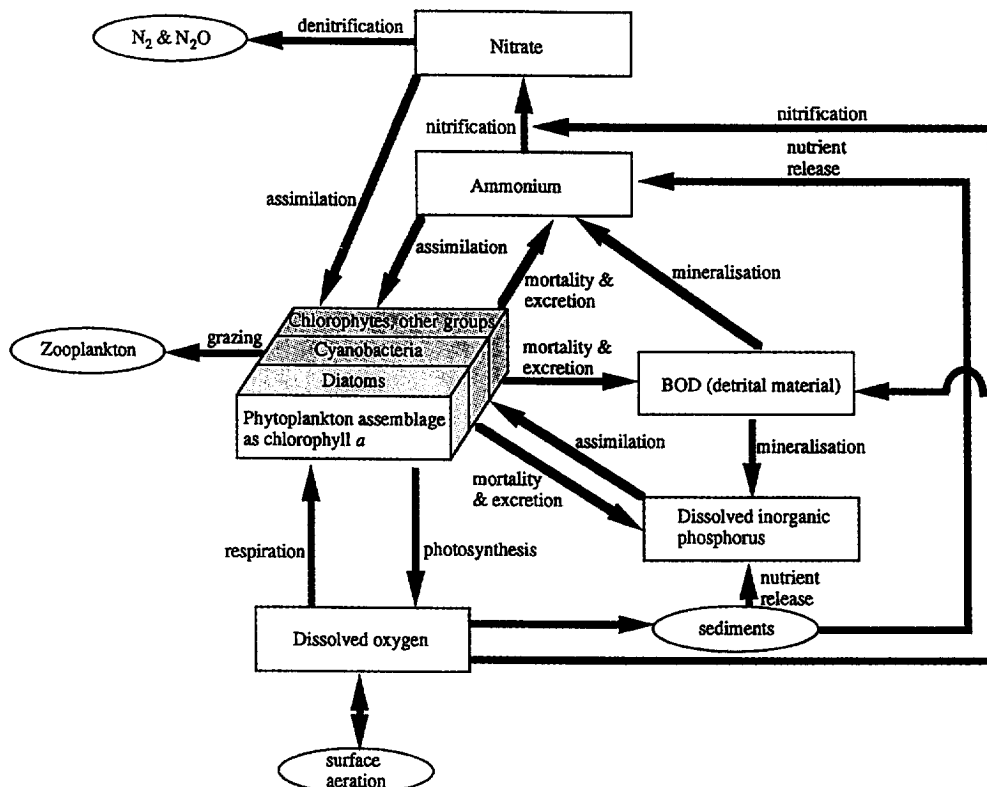


Fig. 3. Relationship between the main state variables, shown in boxes, and the biochemical processes represented in the model. Note that physical processes of inflow, outflow and settling are not included.

nutrients in determining phytoplankton growth is subject to considerable debate (Rhee and Gotham, 1981) and that a number of alternative expressions have been used previously to quantify this interaction (e.g. Di Toro et al., 1971; Cloern, 1978).

The light limitation factor is given by the Steele (1962) function, which includes a photoinhibition

component corresponding to light intensities which exceed the light saturation parameter (Table 3). Inputs of photosynthetically active radiation (PAR) for this model are derived from integrating the short-wave radiation input over each timestep and taking 0.45 of this value to adjust for the photosynthetically active waveband. In addition, a Beer's law formula-

Table 3

Differential equations for the major state variables in the ecological component of the DYRESM Water Quality model. Symbols are given in Table 1

$$\begin{aligned} \frac{\partial P}{\partial t} &= \{G_P \min[g(IP); g(IN); f(I)] - k_r - k_m\} f_P(T) P - K_{gz} f_{gz}(T) Z f_{gz}(P) P \\ g(IP) &= (IP - IP_{\min}) / (IP_{\max} - IP_{\min}) \\ g(IN) &= (IN - IN_{\min}) / (IN_{\max} - IN_{\min}) \\ f(I) &= \frac{I}{I_s} e^{(1-I/I_s)} \\ f_{gz}(P) &= \frac{P}{K_{PZ} + P} \\ \frac{\partial IP}{\partial t} &= \{U_P f(P) f(IP) - k_r IP - k_m IP\} f_P(T) P - K_{gz} f_{gz}(T) f_{gz}(P) IP P \\ \frac{\partial IN}{\partial t} &= \{U_N f(N) f(IN) - k_r IN - k_m IN\} f_P(T) P - K_{gz} f_{gz}(T) f_{gz}(P) IN P \\ \frac{\partial PO_4}{\partial t} &= \{-U_P f(P) f(IP) + k_r IP + k_m (IP - IP_{\min})\} f_P(T) P + K_{gz} f_{gz}(T) f_{gz}(P) P IPE_{gxp} Z + S_P f_s(T) f_s(DO) A + k_{OP} f_B(T) OP \\ f(P) &= PO_4 / (K_P + PO_4) \\ f(IP) &= (IP_{\max} - IP) / (IP_{\max} - IP_{\min}) \\ f_s(DO) &= 1 - [DO / (K_s + DO)] \\ \frac{\partial NH_4}{\partial t} &= \{-U_N f(N) f(IN) P(NH_4) + k_r IN + k_m (IN - IN_{\min})\} f_P(T) P + k_{ON} f_B(T) ON + K_{gz} f_{gz}(T) f_{gz}(P) P INE_{gxp} Z + S_N f_s(T) f_s(DO) A \\ &\quad - k_n f_n(T) f_n(DO) NH_4 \\ f(N) &= (NO_3 + NH_4) / (K_N + NO_3 + NH_4) \\ f(IN) &= (IN_{\max} - IN) / (IN_{\max} - IN_{\min}) \\ P(NH_4) &= \frac{NH_4 NO_3}{(NH_4 + K_N)(NO_3 + K_N)} \frac{NH_4 K_N}{(NH_4 + NO_3)(NO_3 + K_N)} \\ \frac{\partial NO_3}{\partial t} &= -U_N f(N) f(IN) [1 - P(NH_4)] f_P(T) P + k_n f_n(T) f_n(DO) NH_4 - k_d f_d(T) f_d(DO) NO_3 \\ f_d(DO) &= 1 - [DO / (K_{den} + DO)] \\ f_n(DO) &= DO / (K_{nit} + DO) \\ \frac{\partial DO}{\partial t} &= (W/h_s)(C^* - DO_s)^a - k_n f_n(T) f_s(DO) NH_4 Y_{ON} - [k_b f_b(T) f_b(DO)]/h^b \\ &\quad + \{G_P \min[f(IP); f(IN); f(I)] - k_r\} f_P(T) PY_{CC} Y_{OC} - k_{BOD} f_B(T) f_{BOD}(DO) BOD \\ f_{BOD}(DO) &= DO / (K_{BOD} + DO) \\ f_b(DO) &= DO / (K_b + DO) \\ \frac{\partial BOD}{\partial t} &= k_m f_P(T) PY_{OP} - k_{BOD} f_B(T) f_{BOD}(DO) BOD \end{aligned}$$

$f_P(T)$, $f_{gz}(T)$, $f_B(T)$, $f_b(T)$, $f_{gz}(T)$, $f_s(T)$, $f_d(T)$, $f_n(T)$ are temperature functions of form ϑ^{T-20} where T is water temperature and ϑ_p , ϑ_{gz} , ϑ_B , ϑ_b , ϑ_{gz} , ϑ_s , ϑ_d , ϑ_n are non-dimensional temperature multipliers specific for each biochemical process.

^a Applies only when considering surface layer of depth h_s .

^b Applies only when considering sub-euphotic zone, for a layer of depth h .

tion is used to adjust PAR with depth, where the extinction coefficient is determined as

$$\eta = \eta_w + \eta_c P + \eta_s S \quad (12)$$

where η_w is a background extinction coefficient, P is the concentration of chlorophyll *a* for which there is a specific extinction coefficient, η_c (refer to Bannister, 1974a; Bannister, 1974b) and S is the suspended sediment concentration for which a specific extinction coefficient, η_s , is also assigned. The parameter for light saturation of phytoplankton, I_s , is adjusted to a fixed fraction of incoming PAR for the previous two simulation days, to account for photoadaptation (see Ferris and Christian, 1991, for a review of photoadaptation time scales). Maximum and minimum bounds are also assigned to I_s values to correspond to the range of physiological adaptation by phytoplankton.

The model of phosphorus and nitrogen dynamics within phytoplankton cells is designed to account for luxury uptake of these nutrients (Stewart et al., 1978; Rhee and Gotham, 1980). Upper and lower parameter bounds are assigned to the internal nutrients to represent maximum physiological storages and minimum levels required for growth. Silica is a potential growth limiting factor only for diatoms and is therefore included as a state variable only when diatoms are modelled as a discrete group. A simple Michaelis–Menten function is used to determine the silica limitation factor for diatoms within each layer, based on concentrations of dissolved inorganic silica in the layer. Table 3 gives full details of the equations used to parameterise the various biological and chemical reactions represented in the model.

Phytoplankton loss terms include respiration and excretion, natural mortality and zooplankton grazing. The terms for respiration (including excretion) and mortality are modelled in the usual manner as first order losses, with an identical temperature dependence to that for growth. In most cases zooplankton biomass is not included as a separate state variable, generally due to a paucity of data, although a variation of the model has been used to simulate zooplankton distributions (Hamilton and De Stasio, in press). When zooplankton biomass is not modelled explicitly, however, removal of phytoplankton by grazing may still be varied according to chlorophyll *a* concentrations, grazing preferences of zooplankton

and water temperature (e.g. Lehman, 1976). Gravitational settling of phytoplankton is dependent on temperature through its effects on viscosity and density of water. It is treated as a special case in the particle settling model described above. An effective diameter is assigned to the phytoplankton assemblage or to each of the individual phytoplankton groups, so that only the density is adjusted as part of the calibration.

2.8. Nutrients

Uptake of phosphorus and nitrogen by phytoplankton is linked to concentrations of these nutrients internally and to concentrations of the dissolved inorganic nutrients in the water column. The terms that describe loss of phytoplankton by respiration and excretion, mortality and settling are also used to describe losses of internal nutrients. Phytoplankton mortality contributes the minimum assigned internal nutrient pool to the pool of organic nutrients in the water column, while any luxury storages contribute directly to dissolved inorganic phosphorus and ammonium in the water column.

Nitrification and denitrification influence the dissolved inorganic nitrogen fraction, which includes ammonium and nitrate as state variables. These processes are represented as first order, oxygen-dependent reactions (Golterman, 1975). Ammonium and dissolved inorganic phosphorus concentrations are also influenced by release from the sediments, with enhancement of release rates under low oxygen conditions, to account for progressive sediment anoxia (Lee et al., 1977; Nurnberg, 1984).

The organic phosphorus pool available for mineralization is given by the difference between the concentrations of total phosphorus and the sum of dissolved inorganic phosphorus and phytoplankton internal phosphorus. For nitrogen, the organic pool is the difference between the concentrations of total nitrogen and the sum of nitrate, ammonium and phytoplankton internal nitrogen. Settling of each of these nutrient pools is accomplished using the particle settling model described above. Mineralization of the organic nutrient pools back to inorganic nutrients (i.e. dissolved inorganic phosphorus and ammonium) is modelled as a first order, temperature-dependent process.

2.9. Dissolved oxygen

The dissolved oxygen concentration is evaluated as the sum of the following oxygen sources and sinks: surface transfer, inflows and outflows, phytoplankton photosynthesis and respiration, biochemical and sediment oxygen demand, and nitrification. Surface transfer acts as a source of oxygen when surface water concentrations are below saturation and as a sink when they exceed saturation. The saturation concentration of dissolved oxygen (C^*) is determined from the surface water layer temperature, T_s , according to the equation given by Mortimer (1981):

$$C^* = \exp[7.71 - 1.31 \log(T_s + 45.93)] \quad (13)$$

Determination of oxygen flux at the surface–water interface is similar to that described by Patterson et al. (1985) in which a transfer velocity is determined for oxygen exchange at the interface. This transfer velocity is dependent on wind velocity and the resultant wave action, and water viscosity, which is derived from the temperature of the surface water layer.

The equation for the effect of phytoplankton photosynthesis and respiration on the dissolved oxygen concentration is identical to that for changes in chlorophyll *a*, except for the inclusion of a phytoplankton carbon to chlorophyll *a* conversion factor (Ambrose et al., 1988) and a constant stoichiometric factor to convert changes in phytoplankton carbon to dissolved oxygen produced or respired (USCE, 1986). The effect of nitrification on dissolved oxygen is handled similarly, with the equation being identical to that for the effect of nitrification on the nitrate concentration except for a stoichiometric factor to convert nitrate produced to oxygen consumed in the process (USCE, 1986).

Oxygen demand of sediments in the euphotic zone is assumed to be met through primary production associated with benthic production. In the sub-euphotic zone, a modification of the sediment oxygen model of Walker and Snodgrass (1986) is used, so that the sediment oxygen demand in a specific layer is determined from the contact area of the water and the sediments, and the water temperature and dissolved oxygen concentration of the layer.

To model biochemical oxygen demand the detrital mass is considered in terms of its equivalent oxygen consumption. Changes in chlorophyll *a* due to mor-

talinity are therefore converted to an increment in the biochemical oxygen demand using the same conversions of carbon to chlorophyll *a* and oxygen to carbon as those used for the effects of phytoplankton photosynthesis and respiration on dissolved oxygen. The biochemical oxygen demand is reduced through mineralization of the detrital mass via a first order temperature dependence.

2.10. Input requirements

Input requirements for the model are of four types. These are descriptive data for the lake or reservoir itself, hydrodynamic forcing data (primarily meteorological, inflow and outflow), water quality parameters, and initial conditions for all the modelled variables.

The descriptive data for the lake comprise of the hypsography and, in the case of a reservoir, the crest height and the level of all submerged offtakes. The longitudinal slope and the channel cross section of major inflowing streams must be estimated from topographical maps, to calculate inflow entrainment.

The meteorological data requirements are daily averages of wind speed, air temperature and vapor pressure (at known heights above the water surface), daily shortwave radiation, daily rainfall, and a measure of daily longwave radiation, which may come from estimates of cloud cover (Tennessee Valley Authority, 1972) or by direct measurement of the longwave radiation. For the inflow, daily flow volumes for the major streams are required. A water balance calculation using water level, rainfall and outflow volume measurements, and calculations of evaporation (Tennessee Valley Authority, 1972), should be used to account for inflows from ungauged streams, overland flow and groundwater flow. In addition, daily average temperature for the major inflows should be measured or estimated from correlations with air temperature. Likewise, daily volumetric outflow over the spillway, from submerged outlets or from outflowing streams is required. The temperatures of these flows are not required, as they are one of the model output variables. The water quality characteristics of all of the inflows should also be known. These include concentrations of dissolved oxygen, nutrients, BOD, chlorophyll *a* and particles (suspended solids or turbidity). As for tem-

perature, the water quality characteristics of the out-flow water are a model output variable.

To initialize the model, a vertical profile of all the model variables, including water quality variables, must be provided. An initial value of the light extinction coefficient must also be provided.

2.11. Model output

There are presently four main types of output from the model. The first type takes the form of

vertical profiles of any of the model variables. For the hydrodynamic model these profiles would include temperature, salinity and density. For the particle model the profiles include concentrations of particles in the size ranges modelled. For the ecological model the profiles include concentrations of chlorophyll *a* (either for the entire assemblage or by functional group), nutrients and dissolved oxygen. The dissolved oxygen has also been partitioned into individual contributions due to the initial profile,

Table 4
Literature values for major biological and chemical parameters in the DYRESM Water Quality model. The superscripted number above each value or range identifies the source of information. See Table 1 for definitions of parameters

Parameter	Units	Literature values and ranges
G_P	day^{-1}	1.3–2.5 ¹⁸ , 1.6–2.1 ¹⁵ , 1.8 ³⁷ , 1.8–3.9 ³ , 2.0 ^{32,43,17} , 2.1 ³⁴ , 2.3 and 2.53 ^{10,20} , 2.4 ⁶ , 2.5 ¹⁶ , 3.63 ³⁶
k_r	day^{-1}	0.001 ¹⁰ , 0.02–0.16 ⁶ , 0.03 ¹⁵ , 0.05 ²³ , 0.05–0.10 ⁴ , 0.125 ⁴³ , 0.088 and 0.13 ²⁰ , 0.171 ³⁶
k_m	day^{-1}	0.001 ¹⁹ , 0.01–0.03 ³⁸ , 0.015 ¹⁶ , 0.02 ⁴³ , 0.075 ³ , 0.09 ^{10,20} , 0.1 ⁴² , 0.125 ¹⁷
∂_P		1.02 ^{10,17} , 1.045, 1.049 ³⁶ , 1.068 ^{25,43} , 1.08 ^{32,43} , 1.1 ^{28,42} , 1.14 ²¹
I_s	$\mu\text{E m}^{-2} \text{s}^{-1}$	105–697 ¹⁴ , 154–588 ¹⁵ , 158–380 ²⁹ , 194 ³⁴ , 242–290 ²⁷ , 290 ^{1,3} , 290–339 ^{18,19} , 339 ^{10,11} , 500 ^{32,42}
η_C	$\text{m}^2 (\text{mg Chl } a)^{-1}$	0.010 ¹⁹ , 0.01–0.03 ³⁵ , 0.016 ^{5,22} , 0.018 ¹⁷ , 0.019 ⁶ , 0.020 ^{10,36} , 0.022 ²⁶ , 0.03–15.1 ³³
η_W	m^{-1}	0.03–15.1 ³³
IP_{\min}	$\text{mg P (mg Chl } a)^{-1}$	0.1 ^{20,36} , 0.1–0.5 ³⁵ , 1.0 ^{39,42}
IP_{\max}	$\text{mg P (mg Chl } a)^{-1}$	0.95 ³⁶ , 1.3 ²⁰ , 1.3–3.0 ³⁵ , 2.5 ³⁹ , 10.9 ⁴²
IN_{\min}	$\text{mg N (mg Chl } a)^{-1}$	1.5 ²⁰ , 1.5–4 ³⁵
IN_{\max}	$\text{mg N (mg Chl } a)^{-1}$	10 ²⁰ , 8 ³⁶ , 8–15 ³⁵ , 12 ³⁰
U_P	$\text{mg P (mg Chl } a)^{-1} \text{ day}^{-1}$	0.14 and 0.3 ²⁰ , 0.2–1.0 ³⁵ , 0.35 ¹⁷ , 0.5 ³⁶ , 0.6 ³⁰
U_N	$\text{mg N (mg Chl } a)^{-1} \text{ day}^{-1}$	0.96 ¹⁷ , 1–5 ³⁵ , 1.5 and 3 ²⁰ , 2 ³⁶ , 2.3 ³⁰
K_P	mg m^{-3}	1 ³⁴ , 1.4–10.0 ¹⁴ , 2 ³² , 2.5 ¹⁵ , 3 ³⁹ , 4 ³⁷ , 4–10 ²⁷ , 5–30 ³⁵ , 9 ³⁸ , 10 ^{11,40} , 20 ^{10,20}
K_N	mg m^{-3}	0–35 ²⁷ , 15–150 ¹⁴ , 25 ^{1,11,43} , 50–500 ³⁵ , 200 ^{10,20} , 340 ³⁰
ρ_P	kg m^{-3}	1000–1004 ¹⁵ , 1004 ³⁴ , 1004–1018 ²⁴ , 1005–1042 ³⁵ , 1011 ³² , 1015 ³⁰ , 1027–1190 ²⁷
k_n	day^{-1}	0.013 ³¹ , 0.02 ²⁰ , 0.005 ²⁷
k_b	$\text{g m}^{-2} \text{ day}^{-1}$	0.39 ² , 0.58–5.52 ⁴¹ , 1.69 ⁴⁵ , 1.73 ¹²
k_{BOD}	day^{-1}	0.005 ³² , 0.001 ²⁷
k_{OP}	day^{-1}	0.002–0.018 ³⁹ , 0.22 ⁴³ , 0.25 and 0.4 ²⁰ , 0.2–0.8 ³⁰
k_{ON}	day^{-1}	0.024 ³⁶ , 0.03 ¹⁰ , 0.05 ³⁸ , 0.05–0.3 ²⁰ , 0.075 ^{32,43} , 0.1 ³⁰
ρ_T	kg m^{-3}	1.08 ⁴³
ρ_B	kg m^{-3}	1.08 ⁴³
∂_n		1.08 ⁴³
∂_B		1.07 ^{20,36} , 1.08 ^{32,43}
S_P	$\text{mg m}^{-2} \text{ day}^{-1}$	0.02 ⁴² , 0.03–0.8 ²⁷ , 0.27–17 ⁸ , 6.7–40 ³ , 22–49 ⁹
S_N	$\text{mg m}^{-2} \text{ day}^{-1}$	5–15 ¹² , 48 ⁴⁴
∂_S		1.02 ^{10,13} , 1.03 ²⁰

Sources of literature: ¹ Di Toro et al. (1971). ² Burns and Ross (1972). ³ O'Connor et al. (1973). ⁴ Andersen (1974). ⁵ Bannister (1974b). ⁶ Larsen et al. (1974). ⁷ Steele (1974). ⁸ Literature range cited by Bengtsson (1975). ⁹ Measurements by Bengtsson (1975). ¹⁰ Chen and Orlob (1975). ¹¹ Di Toro et al. (1975). ¹² Fillos and Swanson (1975). ¹³ Jørgensen et al. (1975). ¹⁴ Lehman et al. (1975). ¹⁵ Canale et al. (1976). ¹⁶ Gargas (1976). ¹⁷ Jørgensen (1976). ¹⁸ O'Connor et al. (1976). ¹⁹ Scavia and Park (1976). ²⁰ Jørgensen et al. (1978). ²¹ Nyholm (1978). ²² Smith and Baker (1978). ²³ Smith (1979). ²⁴ Burns and Rosa (1980). ²⁵ Di Toro and Matystik (1980). ²⁶ Megard et al. (1980). ²⁷ Scavia (1980). ²⁸ Smith (1980). ²⁹ Belay (1981). ³⁰ Jørgensen et al. (1981). ³¹ Hall (1982). ³² Chapra and Reckhow (1983). ³³ Kirk (1983). ³⁴ Martin et al. (1985). ³⁵ Jørgensen et al. (1986). ³⁶ Matsuoka et al. (1986). ³⁷ Miyanga (1986). ³⁸ USCE (1986). ³⁹ Rossi et al. (1986). ⁴⁰ Virtanen et al. (1986). ⁴¹ Walker and Snodgrass (1986). ⁴² Riley and Stefan (1987). ⁴³ Ambrose et al. (1988). ⁴⁴ Reddy et al. (1988). ⁴⁵ Sweetts et al. (1991).

inflows, a sum for all of the biochemical processes, and surface aeration (Hamilton and Schladow, 1994). The profiles are generally produced once daily, corresponding to solar noon, although they could be produced at every sub-daily timestep to correspond as required to the time of sampling.

The second type of output is for the characteristics of the outflow water. The concentration of any of the modelled variables in either controlled withdrawals or spillway overflow is produced once daily at solar noon.

The third type of output concerns the inflows to the lake. For every day, the level of insertion of any inflow is produced, along with the water quality characteristics of the insertion (a combination of the river inflow and subsequent entrainment).

The fourth type of output concerns the components of the turbulent kinetic energy production equation. At every timestep, the magnitude of each component of these equations can be produced, thus allowing a comparison of the exact source of mixing energy and subsequent hydrodynamic and water quality changes.

3. Model parameters

As a preliminary step to the model calibration, ranges were derived for each of the major model parameters, based on field, laboratory and modelling studies reported in the literature (see Jørgensen et al., 1991 for an extensive review of literature values). Table 4 gives a review of the parameter values and the ranges allocated to each of the parameters for use in the sensitivity analysis described in Part II. The main focus of the literature review of Table 4 was to derive values for parameters that have not already been reviewed by Jørgensen et al. (1991). Structural dynamic modelling (Jørgensen, 1992) is one means whereby parameters may be eliminated or their ranges reduced, but in the initial phase of such a process, literature values are still an essential step prior to laboratory or in situ investigation, to obtain values for critical parameters, and subsequent sensitivity analysis. Table 5 shows additional parameters or stoichiometric factors used in DYRESM Water Quality which were set at fixed values for the model sensitivity analysis and calibration of Part II. To

Table 5

Model parameters and stoichiometric factors that were set at fixed values in the model. See Table 1 for definitions of parameters.

Parameter	Units	Literature values	Assigned value
K_{BOD}	g m^{-3}	0.5 ¹⁸	0.5
K_S	g m^{-3}	0.4 ¹¹	0.4
K_{ON}	g m^{-3}	2.0 ¹⁸	2.0
K_b	g m^{-3}	1.4 ¹³	1.4
Y_{OC}		2.67 ¹⁴	2.67
Y_{ON}		4.57 ¹⁸	4.57
k_Z	day^{-1}	0.18 ⁶ , 0.44 ¹⁴ , 0.6–0.85 ⁸ , 0.85 ¹⁶ , 1.2–1.8 ¹² , 1.3 ⁴	0.5
θ_b		1.085 ¹³	1.08
θ_{gz}		1.045 ¹⁵ , 1.06 ¹⁷ , 1.15 ¹⁶	1.1
$\text{Chl } a_{\min}$	mg m^{-3}	0.1–2.0 ¹² , 1.0 ^{1,17} , 5.0 ⁹ , 10.0 ⁵	1.0
K_{PZ}	mg m^{-3}	1.5–4 ¹² , 1.6–15 ¹ , 5 ^{2,6} , 7 ⁷ , 10 ³ , 40 ¹⁰	5.0

Sources of literature: ¹ Steele (1974). ² Chen and Orlob (1975). ³ Thomann et al. (1975). ⁴ Gargas (1976). ⁵ Lehman (1976). ⁶ Jørgensen (1976). ⁷ O'Connor et al. (1976). ⁸ Scavia and Park (1976). ⁹ Jørgensen et al. (1978). ¹⁰ Nyholm (1978). ¹¹ Bates and Neafus (1980). ¹² Scavia (1980). ¹³ Walker and Snodgrass (1986). ¹⁴ USCE (1986). ¹⁵ Chapra and Reckhow (1983). ¹⁶ Matsuoka et al. (1986). ¹⁷ Riley and Stefan (1987). ¹⁸ Ambrose et al. (1988).

adjust certain literature values to units used in the present study it was assumed that chlorophyll *a* represented 1% of phytoplankton biomass and, for considerations of phytoplankton density, that the mean cell diameter was 20 μm .

4. Discussion

It may be questioned to what extent a one-dimensional model adequately represents a natural system such as a lake or reservoir. From the point of view of the hydrodynamics, provided that the lake is neither extremely long and narrow, nor extremely broad and shallow, a one-dimensional hydrodynamic approach is satisfactory (Orlob, 1983). Gradients in the horizontal directions are generally small when compared to the vertical gradients that exist for much of the year, and are rapidly annihilated by gravitational adjustments. Simple force balances can be used to make a general confirmation of this assumption and to verify its applicability for particular cases (Water Resources Engineering, 1969; Fischer et al., 1979; Imberger and Patterson, 1990).

By contrast, water quality variables, for example nutrient concentrations, exert a negligible effect on the density distribution, and therefore could potentially display a two- or three-dimensional distribution despite a 1D density distribution. While this is recognized as a shortcoming of a 1D model, it does not necessarily imply that a multi-dimensional approach would produce a more correct picture. Indeed, given the difficulty of setting realistic initial conditions for all water quality variables in a multi-dimensional model and the difficulty of knowing all of the input fluxes at the spatial scale of the model, a multi-dimensional predictive capacity (as opposed to a multi-dimensional verification capacity) is a highly uncertain outcome in many natural systems. By explicitly recognizing that the output from a 1D model is a horizontally averaged result, the 1D assumption provides a base level prediction which can be achieved with a greater degree of certainty and from which inferences about possible horizontal distributions can be drawn.

Of greater importance than the dimensionality of the model is the requirement that the hydrodynamic model be process oriented so that it can be based on the correct modelling of the individual mixing processes and not be reliant on site-specific calibration. One could question the need to use a process based hydrodynamic model, given that the ecological components are unavoidably reliant on a large number of calibrated parameters. However, a common use of coupled hydrodynamic and ecological models is to investigate the effects of altered or extreme hydrodynamic forcing conditions (Straškraba, 1994), for which observations and hence calibration information are not available (Schladow and Hamilton, 1995). A process-based hydrodynamic model therefore allows for the identification and description of the set of physical conditions and the process by which a particular water quality outcome has occurred. Unless one is prepared to model by extrapolation, such applications would be beyond the scope of a model that did not explicitly address individual processes. In addition, understanding of lake mixing processes, at least in a horizontally-averaged, one dimensional sense, is sufficient to allow a description of this nature. It therefore greatly simplifies the process of calibration and validation of the water quality component if it is known a priori that the

hydrodynamic representation is site-independent. Such a model thus provides greater information as to what man-made interventions, treatments or alterations in flow regime may produce desirable changes in water quality.

A review of parameters used in the calibration of the biochemical processes represented in the model shows a wide range of values for many of the parameters. This range may reflect, for example, differences in the composition, age structure and physiology of bacterial, phytoplankton or zooplankton communities. It may also represent differences in substrates, e.g., variations in the relative fractions of labile and refractory organic matter, compensatory adjustments for processes that are not represented in the model or parameters that lack physical meaning. It seems likely, therefore, that the biological and chemical parameters will nearly always require calibration for new applications of water quality models which include several state variables. Modelling at the species level is one means of reducing calibration when many of the relevant growth and loss parameters for a species are already well established, but extension of this approach to the lake ecosystem level is still severely limited by the complexity of natural ecosystems and the interactions that occur within them.

5. Conclusion

A coupled hydrodynamic and ecological water quality model, DYRESM Water Quality, is described. This model is a significant advance on previous ones that seek to predict water quality in lakes and reservoirs. This is primarily a result of the fact that the hydrodynamic component of the model (i.e. DYRESM) is process-based to the extent that it requires no calibration for simulations of the vertical density stratification. The ecological component is based on descriptions of phytoplankton production, nutrient cycling and the oxygen budget. These descriptions are, in many cases, not mechanistic and are therefore very sensitive to calibration. A review of the relevant ecological parameters found in the experimental and modelling literature shows a wide range of values, reflecting variations in measurement techniques, algorithm formulations, ecological pro-

cess interactions and community structure. Although the present state of knowledge in eutrophication modelling does not allow a calibration-free representation of the ecology, the architecture of the model is such that as improved sub-models are developed they can be readily incorporated into the present framework (e.g. Patterson et al., 1994). Feedback of intensive data collection, laboratory or in situ experiments to obtain parameter values, and calibration is critical to the development of dynamic models in which the individual ecological processes and their interactions are accurately represented.

Acknowledgements

Funding for this project was provided by the Drinking Water Quality Programme of the Sydney Water Board through Consultancy Z0066. We acknowledge the useful comments and assistance lent by many of the staff at Sydney Water Board and Australian Water Technologies. We thank John Patterson for detailed reviews of earlier drafts and Jörg Imberger, Ian Fisher, Bob Banens, John Ferris, Stuart Mitchell and Peter Cullen for their comments and insights.

References

- Ahlgren, I., Frisk, T. and Kamp-Nielsen, L., 1988. Empirical and theoretical models of phosphorus loading, retention and concentration vs. trophic state. *Hydrobiol.*, 170: 285–303.
- Ambrose, Jr., R.B., Wool, T.A., Connolly J.P. and Schanz, R.W., 1988. WASP4, a hydrodynamic and water quality model – model theory, user's manual, and programmer's guide, U.S. EPA Report EPA/600/3-87/039, 297 pp.
- Andersen, V.J.M., 1974. Nitrogen and phosphorus budgets and the role of sediments in six shallow Danish lakes. *Arch. Hydrobiol.*, 74: 528–550.
- Bannister, T.T., 1974a. A general theory of phytoplankton growth in a nutrient saturated mixed layer. *Limnol. Oceanogr.*, 19: 13–30.
- Bannister, T.T., 1974b. Production equations in terms of chlorophyll concentration, quantum yield and upper limit to production. *Limnol. Oceanogr.*, 19: 1–12.
- Bates, M.H. and Neafus, N.J.E., 1980. Phosphorus release from sediments from Lake Carl Blackwell, Oklahoma. *Water Res.*, 14: 1477–1481.
- Belay, A., 1981. An experimental investigation of inhibition of phytoplankton photosynthesis at lake surfaces. *New Phytol.*, 89: 61–74.
- Bengtsson, L., 1975. Phosphorus release from a highly eutrophic lake sediment. *Verh. Internat. Verein. Limnol.*, 19: 1107–1116.
- Bloss, S. and Harleman, D.R.F., 1980. Effects of wind induced mixing on the seasonal thermocline in lakes and reservoirs. In: I.T. Carstens and T. McClimans (Editors), 2nd International Symposium on Stratified Flows, Vol. I, Trondheim, Norway.
- Burns, N.M. and Rosa, F., 1980. In situ measurements of settling velocity of organic carbon particles and 10 species of phytoplankton. *Limnol. Oceanogr.*, 25: 855–864.
- Burns, N.M. and Ross, C., 1972. Oxygen–nutrient relationships within the central basin of Lake Erie. U.S.EPA Tech. Rep., TS-05-71-208-24, 85–119.
- Canale, R.P., De Palma, L.M. and Vogel, A.H., 1976. A plankton-based food web model for Lake Michigan. In: R.P. Canale (Editor), *Modeling Biochemical Processes in Aquatic Ecosystems*. Ann Arbor Science, MI, pp. 33–74.
- Canfield, Jr., D.E. and Bachmann, R.W., 1981. Prediction of total phosphorus concentrations, chlorophyll *a* and Secchi depths in natural and artificial lakes. *Can. J. Fish. Aquat. Sci.*, 38: 414–423.
- Canfield, Jr., D.E. and Hoyer, M.V., 1988. The eutrophication of Lake Okeechobee. In: G. Redfield (Editor), *Lake Reservoir Manage.*, 4: 91–100.
- Casamitjana, X. and Schladow, S.G., 1993a. The seasonal cycle of a groundwater dominated lake. *IAHR J. Hydr. Res.*, 31(3): 293–306.
- Casamitjana, X. and Schladow, S.G., 1993b. Vertical distribution of particles in a stratified lake. *J. Env. Eng. ASCE*, 119(3): 443–462.
- Chapra, S.C. and Reckhow, K.H., 1983. *Engineering approaches for lake management*, Vol. 2: Mechanistic modeling. Butterworth, Boston, 492 pp.
- Chen, C.W. and Orlob, G.T., 1975. Ecological simulation for aquatic environments. In: B.C. Patten (Editor), *Systems analysis and simulation in ecology*, Vol. 3. Academic Press, New York, pp. 476–588.
- Cloern, J.E., 1978. Simulation model of *Cryptomonas ovata* population dynamics in Southern Kootenay Lake, British Columbia. *Ecol. Modelling*, 4: 237–252.
- Dake, J.M.K. and Harleman, D.R.F., 1966. An analytical and experimental investigation of thermal stratification in lakes and ponds. R.M. Parsons Laboratory Technical Report, 99. MIT Dept Civil Engineering, 271 pp.
- Dillon, P.J. and Rigler, F.H., 1975. A simple method for predicting the capacity of a lake for development based on lake trophic status. *Can. J. Fish. Res.*, 32: 1519–1531.
- Di Toro, D.M., O'Connor, D.J. and Thomann, R.V., 1971. A dynamic model for the phytoplankton population in the Sacramento San Joaquin Delta. *Adv. Chem. Ser.*, 106: 131–180.
- Di Toro, D.M., O'Connor, D.J., Thomann, R.V. and Mancini, J.L., 1975. Phytoplankton–zooplankton interaction model for Lake Erie. In: B.C. Patten (Editor), *Systems analysis and simulation in ecology*, Vol. 3. Academic Press, New York, pp. 423–474.
- Di Toro, D.M. and Matystik, W.F., 1980. Mathematical models of water quality in large lakes, Part 1: Lake Huron and Saginaw Bay. U.S. EPA Report, EPA-600/3-80-056.

- Ferris, J.M. and Christian, R., 1991. Aquatic primary productivity in relation to microalgal responses to changing light: A review. *Aq. Sci.*, 53: 187–217.
- Fillos, J. and Swanson, W.R., 1975. The release rate of nutrients from river and lake sediments. *J. Water Poll. Control Fed.*, 47: 1032–1041.
- Fischer, H.B., List, E.J., Koh, R.C.Y., Imberger, J. and Brooks, N.H., 1979. Mixing in inland and coastal waters. Academic Press, New York, 483 pp.
- Forsberg, C., 1987. Evaluation of lake restoration in Sweden. *Scheiz. Z. Hydrol.*, 49: 260–274.
- Gargas, E., 1976. A three-box eutrophication model of a mesotrophic Danish lake. Water Quality Institute, Hørsholm, Denmark.
- Golterman, H.L., 1975. *Physiological limnology*. Elsevier Science Publ., Amsterdam, 489 pp.
- Hall, G.H., 1982. Apparent and measured rates of nitrification in the hypolimnion of a mesotrophic lake. *Appl. Env. Microbiol.*, 43: 542–547.
- Hamilton, D.P. and Schladow, S.G., 1994. Modelling the sources of oxygen in an Australian Reservoir. *Verh. Internat. Verein. Limnol.*, 25: 1282–1285.
- Hamilton, D.P. and De Stasio, B.T. (in press). Modelling phytoplankton–zooplankton interactions in Sparkling Lake. *Verh. Internat. Verein. Limnol.*, 26.
- Hocking, G.C., Sherman, B.S. and Patterson, J.C., 1988. An algorithm for selective withdrawal from a stratified reservoir. *J. Hydr. Div., ASCE*, 114: 707–719.
- Imberger, J., 1982. Reservoir dynamics modelling. In: E.M. O’Laughlin and P. Cullen (Editors), *Predictions in Water Quality*. Aust. Acad. Sci., Canberra, pp. 223–248.
- Imberger, J. and Patterson, J.C., 1981. A dynamic reservoir simulation model – DYRESM: 5. In: H.B. Fischer (Editor), *Transport models for inland and coastal waters*. Academic Press, New York, pp. 310–361.
- Imberger, J. and Patterson, J.C., 1990. *Physical limnology*. Adv. Appl. Mech., 27: 303–475.
- Imberger, J., Patterson, J.C., Hebbert, B. and Loh, I., 1978. Dynamics of reservoirs of medium size. *J. Hydr. Div., ASCE*, 104: 725–743.
- Imberger, J., Thompson, R. and Fandry, C., 1976. Selective withdrawal from a finite rectangular tank. *J. Fluid Mech.*, 78(3): 489–512.
- Jokela, J.B. and Patterson, J.C., 1985. Quasi-two-dimensional modelling of reservoir inflow. *Proceedings, 21st Congress International Association Hydraulic Research (IAHR)*, Melbourne.
- Jørgensen, S.E., 1976. A eutrophication model for a lake. *Ecol. Modelling*, 2: 147–165.
- Jørgensen, S.E., 1983. Eutrophication models of lakes. In: S.E. Jørgensen (Editor), *Application of ecological modelling in environmental management, part A*. Elsevier Sci. Publ., Amsterdam, pp. 227–282.
- Jørgensen, S.E., 1992. *Integration of ecosystem theories: A pattern*. Kluwer Academic Publ., The Netherlands, 383 pp.
- Jørgensen, S.E., Kamp-Nielsen, L. and Jacobsen, O.S., 1975. A submodel for anaerobic mud-water exchange of phosphate. *Ecol. Modelling*, 1: 133–146.
- Jørgensen, S.E., Mejer, H.F. and Friis, M., 1978. Examination of a lake model. *Ecol. Modelling*, 4: 253–279.
- Jørgensen, S.E., Jørgensen, L.A., Kamp-Nielsen, L. and Mejer, H.F., 1981. Parameter estimation in eutrophication modelling. *Ecol. Modelling*, 13: 111–129.
- Jørgensen, S.E., Kamp-Nielsen, L. and Jørgensen, L.A., 1986. Examination of the generality of eutrophication models. *Ecol. Modelling*, 32: 251–266.
- Jørgensen, S.E., Nielsen, S.N. and Jørgensen, L.A., 1991. *Handbook of ecological parameters and ecotoxicology*. Elsevier, Amsterdam, 1263 pp.
- Kirk, J.T.O., 1983. *Light and photosynthesis in aquatic ecosystems*. Cambridge University Press, 401 pp.
- Kmet, T., Straškraba, M. and Mauersberger, P., 1993. A mechanistic model of the adaptation of phytoplankton photosynthesis. *Bull. Mathemat. Biol.*, 55(2): 259–275.
- Kreith, F. and Kreider, J.F., 1978. *Principles of solar engineering*. Kingsport Press Inc., Washington, 778 pp.
- Larsen, D.P., Mercier H.T. and Malveg, K.W., 1974. Modeling algal growth dynamics in Shagawa Lake, Minnesota. In: E.J. Middlebrooks, D.H. Falkenberg and T.E. Maloney (Editors): *Modeling the eutrophication process*. Ann Arbor Science, MI, pp. 15–33.
- Lee, G.F., Sonzogni, W.C. and Spear, R.D., 1977. Significance of oxic vs anoxic conditions for Lake Mendota sediment phosphorus release. H.L. Golterman (Editor), *Interactions between sediments and freshwater*. The Hague, Netherlands, pp. 294–306.
- Lehman, J.T., 1976. The filter-feeder as an optimal forager, and the predicted shapes of feeding curves. *Limnol. Oceanogr.*, 21: 501–516.
- Lehman, T.D., Botkin, D.B. and Likens, G.E., 1975. The assumptions and rationales of a computer model of phytoplankton population dynamics. *Limnol. Oceanogr.*, 20: 343–364.
- Martin, S.C., Effler, S.W., DePinto, J.V., Trama, F.B., Rodgers, P.W., Dobi, J.S. and Wodka, M.W., 1985. Dissolved oxygen model for a dynamic reservoir. *J. Env. Eng., ASCE*, 111, 647–664.
- Matsuoka, Y., T. Goga and Naito, M., 1986. An eutrophication model of Lake Kasumigaura. *Ecol. Modelling*, 31: 201–219.
- Megard, R.O., Comles, W.S., Smith, P.D. and Knoll, A.S., 1980. Attenuation of light and daily integral rates of photosynthesis attained by planktonic algae. *Limnol. Oceanogr.*, 24: 1038–1050.
- Miyanga, Y., 1986. Modelling of stratified flow and eutrophication in reservoirs. *Ecol. Modelling*, 3: 133–144.
- Mortimer, C.H., 1981. The oxygen content of air-saturated freshwaters over ranges of temperature and atmospheric pressure of limnological interest. *Mitt. Int. Verein. Limnol.*, 21: 1–23.
- Mueller, D.K., 1982. Mass balance model for estimation of phosphorus concentrations in reservoirs. *Water Res. Bull.*, 18: 377–382.

- Numberg, G.K., 1984. The prediction of internal phosphorus load in lakes with anoxic hypolimnia. *Limnol. Oceanogr.*, 29: 111–124.
- Nyholm, N., 1978. A simulation model for phytoplankton growth and nutrient recycling in eutrophic shallow lakes. *Ecol. Modelling*, 4: 279–310.
- O'Connor, D.J., Di Toro, D.M. and Thomann, R.V., 1973. Dynamic water quality forecasting and management. U.S. EPA Report, EPA-660/3-73-009.
- O'Connor, D.J., Thomann, R.V. and Di Toro, D.M., 1976. Ecologic models. In: V. Biswas (Editor): *Systems approach to water management*. McGraw-Hill, New York, pp. 299–333.
- OECD, 1982. Eutrophication of waters. Monitoring, assessment and control. Organisation for Economic Co-operation and Development, Paris, 154 pp.
- O'Melia, C.R., 1980. Aquasols: The behavior of small particles in aquatic systems. *Env. Sci. Tech.*, 14: 1052–1060.
- O'Melia, C.R., 1990. Kinetics of colloid chemical processes in aquatic systems. In: W. Stumm (Editor), *Aquatic chemical kinetics*. John Wiley and Sons, pp. 447–474.
- Orlob, G.T., 1983. One dimensional models for simulation of water quality in lakes and reservoirs. In: G.T. Orlob and G.T. John (Editors), *Mathematical Modeling of Water Quality: Streams, Lakes and Reservoirs*. International Series on Applied Systems Analysis. John Wiley and Sons, pp. 227–273.
- Orlob, G.T. and Selna, L., 1970. Temperature variations in deep reservoirs. *J. Hydr. Div., ASCE*, 96(HY2): Paper 7063.
- Patten, B.C., Egloff, D.A. and Richardson, D.H., 1975. Total ecosystem model for a cove in Lake Texocoma. In: B.C. Patten (Editor), *Systems analysis and simulation in ecology*, Vol. 3. Academic Press, New York, pp. 206–423.
- Patterson, J.C., Hamblin, P.F. and Imberger, J., 1984. Classification and dynamic simulation of the vertical density structure of lakes. *Limnol. Oceanogr.*, 29: 845–861, 1984.
- Patterson, J.C., Allanson, B.R. and Ivey, G.N., 1985. A dissolved oxygen budget model for Lake Erie in summer. *Freshwat. Biol.*, 15: 683–695.
- Patterson, J.C., D.P. Hamilton and Ferris, J.M., 1994. Modelling of algal growth in the mixed layer of lakes and reservoirs. *Aust. J. Mar. Freshwat. Res.*, 45: 829–845.
- Reddy, K.R., Jessup, R.E. and Rao, P.S.C., 1988. Nitrogen dynamics in a eutrophic lake sediment. *Hydrobiologia*, 159: 177–188.
- Rhee, G.-Y. and Gotham, I.J., 1980. Optimum N:P ratios and coexistence in phytoplankton. *J. Phycol.*, 16: 486–489.
- Rhee, G.-Y. and Gotham, I.J., 1981. The effects of environmental factors on phytoplankton growth: Light and the interaction of light with nitrate limitation. *Limnol. Oceanogr.*, 26: 649–659.
- Riley, M.J. and Stefan, H.G., 1987. Dynamic lake water quality simulation model "MINLAKE". St. Anthony Falls Hydr. Lab. Proj. Rep., 263. University of Minnesota, 140 pp.
- Riley, M.J. and Stefan, H.G., 1988. MINLAKE: A dynamic lake water quality simulation model. *Ecol. Modelling*, 43: 155–182.
- Rossi, G., Premazzi, G. and Marengo, G., 1986. Correlation of a lake eutrophication model to field experiments. *Ecol. Modelling*, 34: 167–189.
- Scavia, D., 1980. An ecological model of lake Ontario. *Ecol. Modelling*, 8: 49–78.
- Scavia, D. and Park, R.A., 1976. Documentation and selected constructs in the aquatic model CLEANER. *Ecol. Modelling*, 2: 33–58.
- Schladow, S.G. and Hamilton, D.P., 1995. Modelling sediment nutrient release in a stratified reservoir. *J. Mar. Freshwat. Res.*, 46(1): 189–195.
- Sherman, F.S., Imberger J. and Corcos, G.M., 1978. Turbulence and mixing in stably stratified waters. *Ann. Rev. Fluid Mech.*, 10: 267–288.
- Smith, R.A., 1980. The theoretical basis for estimating phytoplankton production and specific growth rate from chlorophyll, light and temperature data. *Ecol. Modelling*, 10: 243–264.
- Smith, V.H., 1979. Nutrient dependence of primary productivity in lakes. *Limnol. Oceanogr.*, 24: 1051–1064.
- Smith, R.C. and Baker, K.S., 1978. The bio-optical state of ocean waters and remote sensing. *Limnol. Oceanogr.*, 23: 247–259.
- Steele, J.H., 1962. Environmental control of photosynthesis in the sea. *Limnol. Oceanogr.*, 7: 137–150.
- Steele, J.H., 1974. *The structure of marine ecosystems*. Blackwell Scientific Publications, Oxford, 128 pp.
- Stefan, H. and Ford, D.E., 1975. Temperature dynamics in dimictic lakes. *J. Hydr. Div., ASCE*, Paper 11058: 97–114.
- Straškraba, M., 1994. Ecotechnological models of reservoir water quality management. *Ecol. Modelling*, 74: 1–38.
- Stewart, W.D.P., Pemble, M. and Al-Ugaily, L., 1978. Nitrogen and phosphorus storage and utilization in blue-green algae. *Freshwat. Biol.*, 1: 389–404.
- Sweerts, J.-P.R.A., Bär-Gilissen, M.-J., Cornelese, A.A. and Capenberg, T.E., 1991. Oxygen-consuming processes at the profundal and littoral sediment-water interface of a small meso-eutrophic lake (Lake Vechten, The Netherlands). *Limnol. Oceanogr.*, 36: 1124–1133.
- Tennessee Valley Authority, 1972. Heat and mass transfer between a water surface and the atmosphere. *Water Res. Rep.*, 14(0-6803). Noris, Tenn.
- Thomann, R.V., Di Toro, D.M., Winfield, R.P. and O'Connor, D.J., 1975. Mathematical modelling of phytoplankton in Lake Ontario, Part 1: Model development and verification. U.S. Environmental Protection Agency Report, EPA-660/3-75-005.
- USCE, 1986. CE QUAL R1: A numerical one-dimensional model of reservoir water quality, user's manual. Environmental and water quality operational studies instruction report E-82-1. Department of the Army, U.S. Corps Engineers, Washington, DC, 427 pp.
- Vincent, W.F., Gibbs, M.M. and Spiegel, R.H., 1991. Eutrophication processes regulated by a plunging river inflow. *Hydrobiologia*, 226: 51–63.
- Virtanen, M., Kopenen, J., Dahlbo, K. and Sarkkula, J., 1986. Three-dimensional water quality-transport model compared with field observations. *Ecol. Modelling*, 31: 185–199.
- Walker, R.R. and Snodgrass, W.J., 1986. Model for sediment oxygen demand in lakes. *J. Hydraul. Eng., ASCE*, 112: 25–43.
- Watanabe, M., Harleman, D.R.F. and Vasiliev, O.F., 1983. Two- and three-dimensional mathematical models for lakes and

- reservoirs. In: G.T. Orlob and G.T. John (Editors), *Mathematical Modeling of Water Quality: Streams, Lakes and Reservoirs*. International Series on Applied Systems Analysis. John Wiley and Sons, pp. 274–336.
- Water Resources Engineering, Inc., 1969. *Mathematical models for prediction of thermal energy changes in impoundments*. U.S. Environmental Protection Agency Water Pollution Control Research Series, 157 pp.
- Weinstock, J., 1981, Vertical turbulence diffusivity for weak or strong stable stratification. *J. Geophys. Res.*, 86(C10): 9925–9928.